

# Supporting Information

## Determination of Electroactive Surface Area of Ni-, Co-, Fe-, and Ir-based Oxide Electrocatalysts

*Sebastian Watzele<sup>†</sup>, Pascal Hauenstein<sup>†</sup>, Yunchang Liang<sup>‡</sup>, Song Xue<sup>‡</sup>, Johannes Fichtner<sup>‡</sup>, Batyr Garlyyev<sup>‡</sup>, Daniel Scieszka<sup>‡</sup>, Fabien Claudel<sup>⊥</sup>, Frédéric Maillard<sup>⊥</sup>, Aliaksandr S. Bandarenka<sup>‡,\*</sup>*

<sup>†</sup> Physics of Energy Conversion and Storage, Technical University of Munich, James-Franck-Straße 1,  
85748 Garching, Germany

<sup>‡</sup> Catalysis Research Center TUM, Ernst-Otto-Fischer-Straße 1, 85748 Garching, Germany

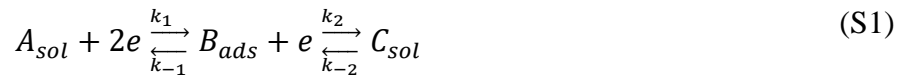
<sup>⊥</sup> University Grenoble Alpes, University Savoie Mont Blanc, CNRS, Grenoble INP, LEPMI, 38000  
Grenoble, France

\* Corresponding author, E-mail: [bandarenka@ph.tum.de](mailto:bandarenka@ph.tum.de) Phone: +49 (0) 89 289 12531

## S1. Justification of the EEC

The following discussion is based on references [1] and [2]. An ideally polarizable electrode can be described by a capacitance,  $C_{dl}$ , in series to the resistance of the electrolyte,  $R_s$ . However, the response of the double layer at an electrode is typically not perfectly capacitive and, therefore, it is often represented by a constant phase element  $Z_{dl} = \frac{1}{Q_0 \omega^n} e^{-\frac{\pi}{2}nj}$ , where  $n$  ( $0 < n < 1$ ) is the phasor and  $\omega$  is the angular frequency. Faradaic reactions are accounted by a Faradaic impedance,  $Z_f$ , which is in parallel to  $Z_{dl}$ .

For a reaction during which in the first step the reactant is adsorbed and in a second step desorbed:



the rates of both reactions in steady-state can be described (under the assumption of Langmuir adsorption isotherm) by:

$$v_1 = k_1^0 \Gamma_\infty C_A(0)(1 - \theta_B) \exp[-\beta_1 f(E - E_1^0)] - k_{-1}^0 \Gamma_\infty \theta_B \exp[(1 - \beta_1)f(E - E_1^0)] \quad (S2)$$

$$v_2 = k_2^0 \Gamma_\infty \theta_B \exp[-\beta_2 f(E - E_2^0)] - k_{-2}^0 \Gamma_\infty C_C(0) \exp[(1 - \beta_2)f(E - E_2^0)] \quad (S3)$$

Here  $k_{1,2}^0$  are the rate constants,  $\Gamma_\infty$  is the total surface concentration of active sites,  $C_{A,C}(0)$  are the concentration of species  $A$  and  $C$  at the surface,  $\theta_B$  is the fractional coverage of the active centers with species  $B$ ,  $\beta_{1,2}$  are the transfer coefficients,  $E$  is the applied potential, and  $E_{1,2}^0$  are the standard potentials for both reactions. Further,  $f = F/RT$ , where  $F$ ,  $R$  and  $T$  are the Faraday constant, the gas constant and the temperature, respectively.

At the equilibrium potential,  $E_{eq}$ , both reaction rates are zero resulting in:

$$\exp[f(E_{eq} - E_1^0)] = \frac{k_1^0}{k_{-1}^0} C_A^* \frac{1 - \theta_B^*}{\theta_B^*} \quad (S4)$$

$$\exp[f(E_{eq} - E_2^0)] = \frac{k_2^0}{k_{-2}^0} C_c^* \frac{\theta_B^*}{1 - \theta_B^*} \quad (S5)$$

Here  $C_{A,C}^*$  are the bulk and  $\theta_B^*$  the surface concentrations at the equilibrium potential. One can rewrite equations (S2) and (S3) several times by introducing an over potential  $E - E_i^0 = E - E_{eq} + E_{eq} - E_i^0 = \eta + E_{eq} - E_i^0$ , assuming that the surface and bulk concentrations are almost identical, which holds for low currents and relatively high electrolyte concentrations. For the detailed calculations, we want to refer to A. Lasia<sup>1</sup>. Summing up the two reactions, the total current can be expressed as:

$$i = -F(v_1 + v_2) = -Fr_0 \quad (S6)$$

and the change of the coverage of surface by species  $B$  can be shown as:

$$\frac{d\Gamma_B}{dt} = \Gamma_\infty \frac{d\theta_B}{dt} = \frac{\sigma_1}{F} \frac{d\theta_B}{dt} = r_1 = v_1 - v_2 = 0 \quad (S7)$$

Here,  $\sigma_1 = F\Gamma_\infty$  is the charge of a totally covered electrode surface.

Linearization of the equations for the total current and changes in the surface coverage results in differential equations with the solution being the Faradaic admittance. The inverse is the Faradaic impedance which can be written as:

$$Z_F = R_{ct} + \frac{1}{j\omega C_a + \frac{1}{R_a}} \quad (S8)$$

With adsorption capacitance and resistance in parallel and a charge transfer resistance in series.

By combining it with the impedance of the double layer and the uncompensated solution resistance, one can see that the total impedance is:

$$Z_{total} = R_U + \frac{1}{Q_0(j\omega)^n + \frac{1}{R_{ct} + \frac{1}{j\omega C_a + \frac{1}{R_a}}}} \quad (S9)$$

and can be represented as the equivalent circuit shown in **Fig. 2B**.

Noteworthy, this Faradaic impedance (S8) was originally found for the Volmer-Heyrovsky pathway of the hydrogen evolution reaction, as it involves one adsorbed intermediate. In general for a reaction with three binding intermediates, all of them need to be taken into account, resulting in a much more complex system of differential equations and an equivalent circuit with more branches. However, assuming that at small overpotential only one OER intermediate step is quasi-reversible (most likely involving the  $\ast\text{OH}$  intermediate), the surface concentration of mainly one specifically adsorbed species varies with the applied potential justifies the choice of this rather simplified circuit. Moreover, the good fitting quality of the impedance data (**Figure S1**) combined with the fact that just one set of parameters can fully fit the experimental findings speaks for the choice of this EEC.

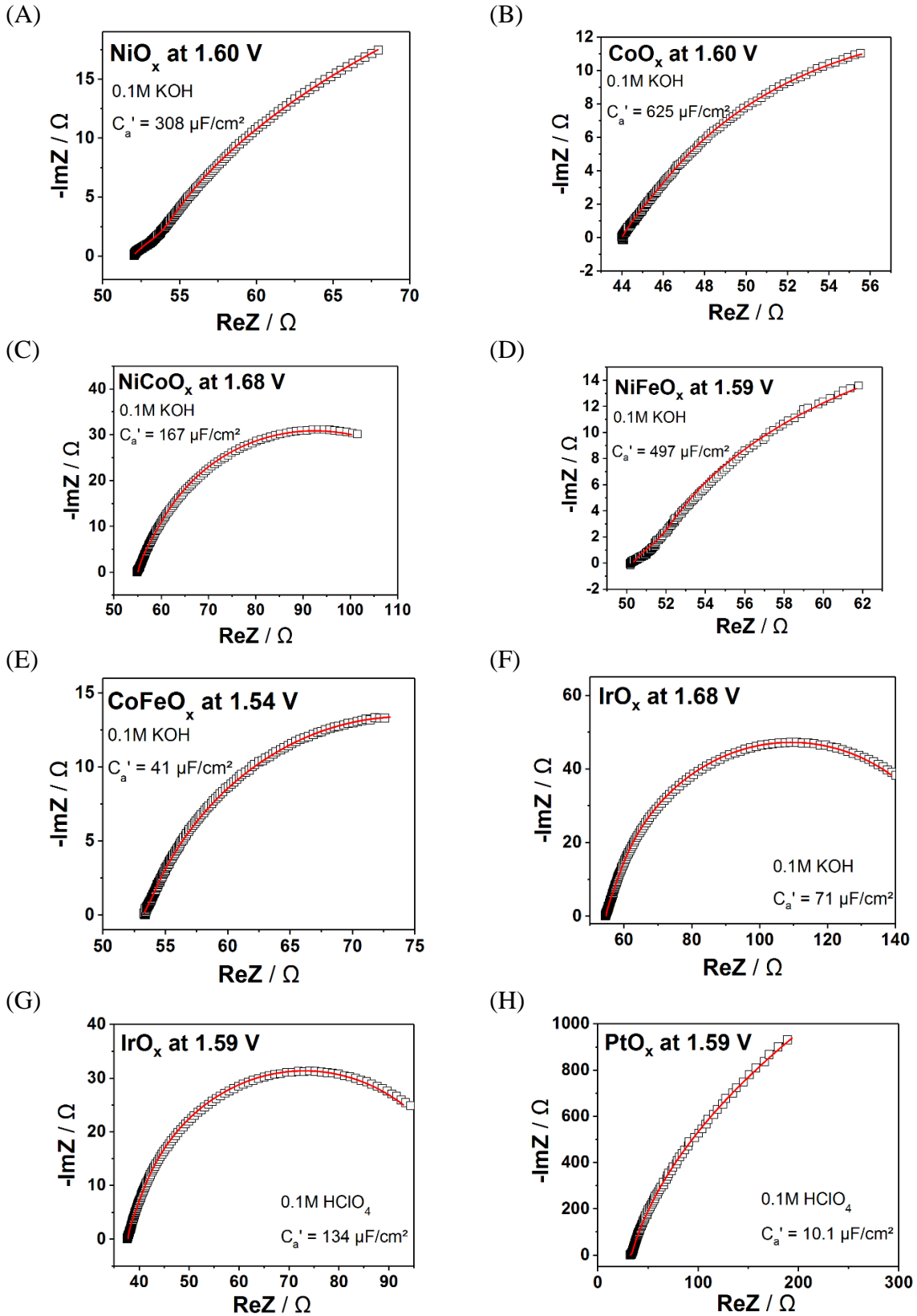


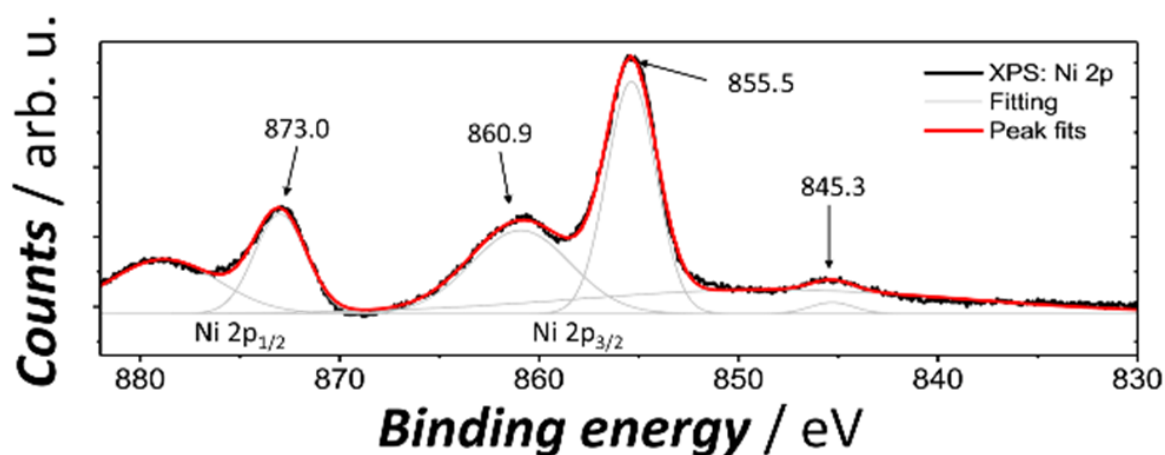
**Figure S1.** (A-G) Nyquist plots (obtained at the potentials indicated in Table 1) of the different oxide materials together with their fits (red lines) obtained using the EEC shown in Fig. 2B.

## S2. X-ray photoelectron spectroscopy (XPS)

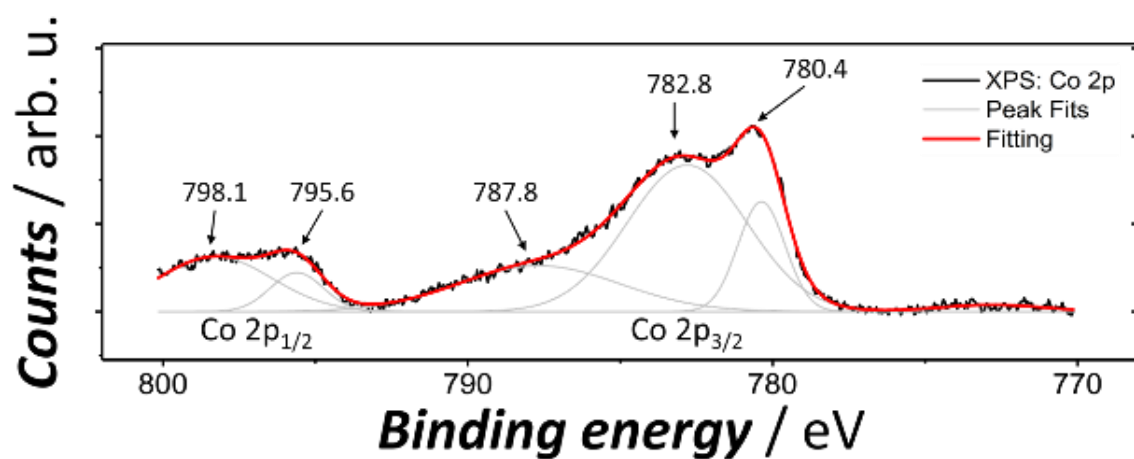
X-ray photoelectron spectra of the *as prepared* catalyst films are shown in Figure S2. The NiO<sub>x</sub> named film consists of Ni(OH)<sub>2</sub> and NiOOH phase and the, as CoO<sub>x</sub> denoted film consists of Co(OH)<sub>2</sub> and CoOOH. The NiFeO<sub>x</sub> film right after the deposition contains additionally to the Ni<sup>II</sup>, Ni<sup>III</sup>, Fe<sup>II</sup>, and the Fe<sup>III</sup> a small amount of metallic Ni<sup>0</sup> and Fe<sup>0</sup> phase. The Ni / Fe ratio was calculated to be 7 / 3 which is close to the optimum of 3 / 1. The spectra taken from the CoNiO<sub>x</sub> film is well comparable to those taken from the NiO<sub>x</sub> and CoO<sub>x</sub> films; however, the binding energies are slightly shifted, indicating an alloyed phase. The Ni / Co ratio is approximately 1 / 1. The film denoted as CoFeO<sub>x</sub> shows mainly Co<sup>II</sup>, Co<sup>III</sup>, Fe<sup>II</sup>, and the Fe<sup>III</sup> oxy-hydroxide phase but also a small fraction of metallic (~5 %) phase. These observed metallic phases are due to the cathodic deposition method. Notably, in the alkaline electrolyte, the metallic fraction of the surface quickly oxidizes during cycling. The 4f<sub>5/2</sub> and 4f<sub>7/2</sub>, observed from the spectra of the IrO<sub>x</sub> named film, confirm the presence of a thin IrO<sub>x</sub> layer covering the Ir-crystal[3],[4].

### Beginning of Figure S2:

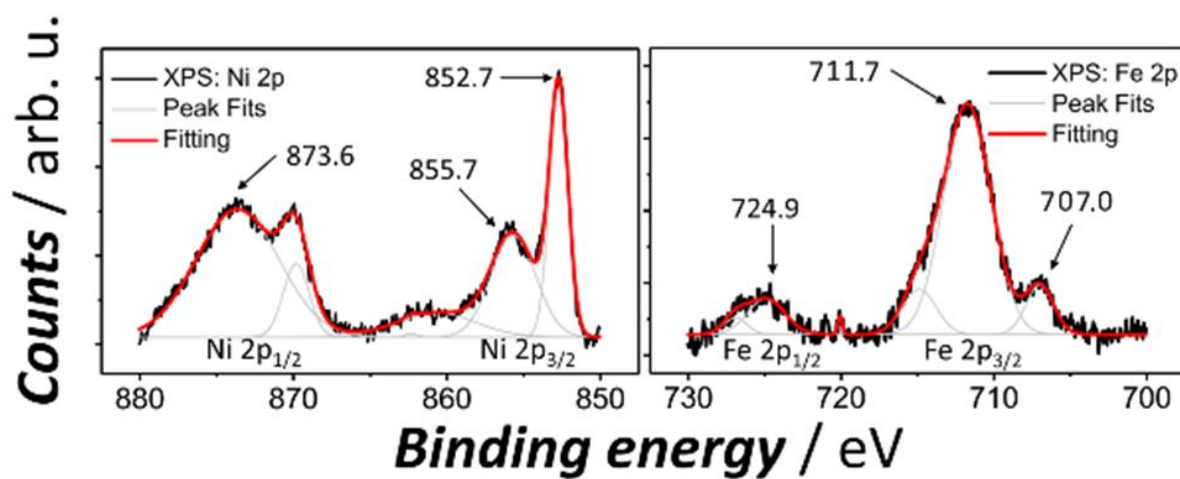
(A) NiO<sub>x</sub>



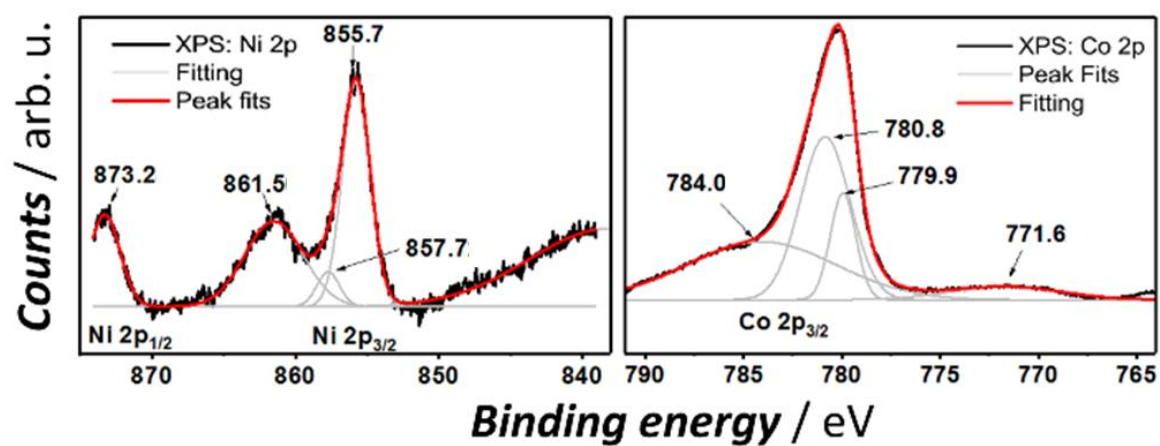
(B)  $\text{CoO}_x$



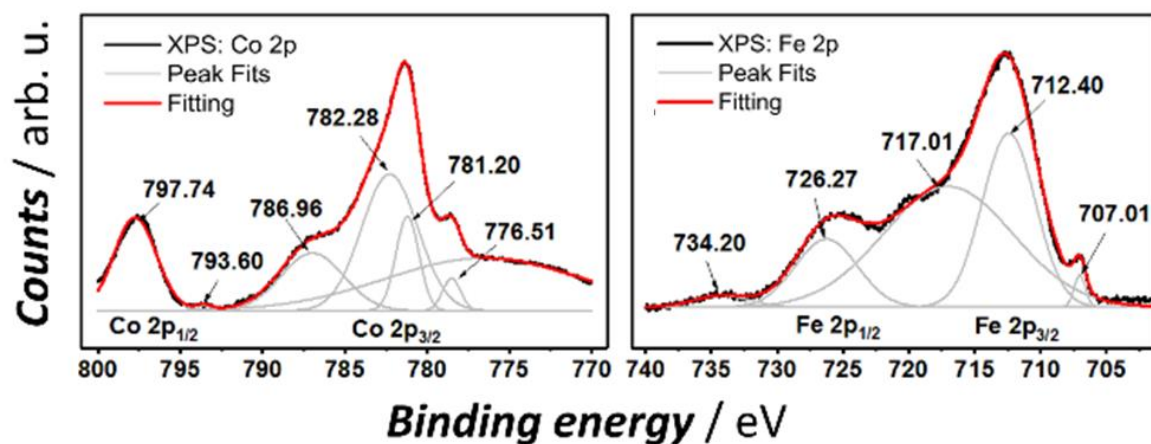
(C)  $\text{NiFeO}_x$



(D)  $\text{CoNiO}_x$



(E)  $\text{CoFeO}_x$



(F)  $\text{IrO}_x$

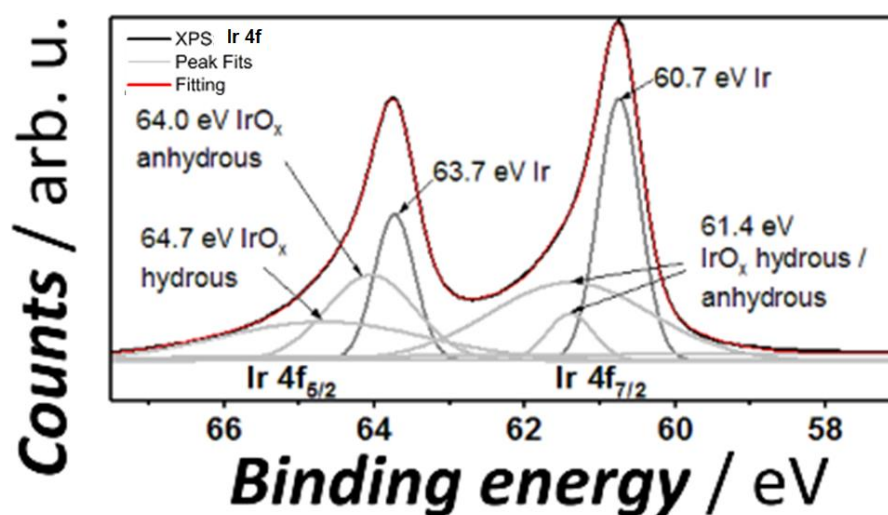


**Figure S2.** XPS of (A)  $\text{NiO}_x$ , (B)  $\text{CoO}_x$ , (C)  $\text{NiFeO}_x$ , (D)  $\text{CoNiO}_x$ , (E)  $\text{CoFeO}_x$ , (F)  $\text{IrO}_x$ . Figures (A-C) are adapted with permission from ref. [5].

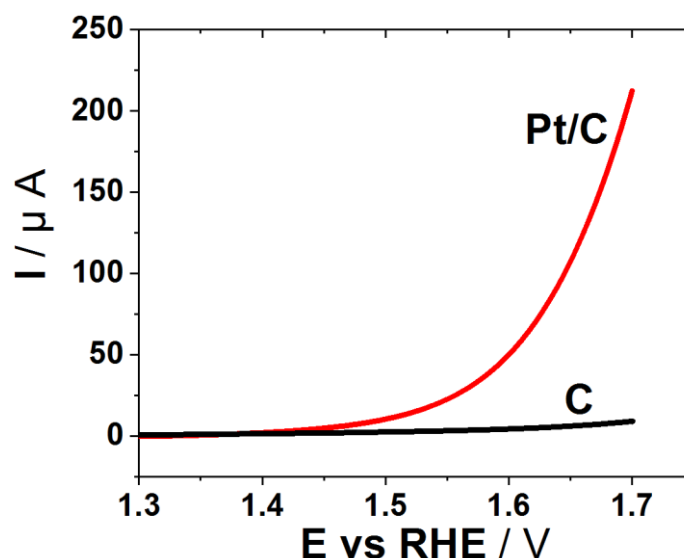


**Figure S3.** Anodic voltammetric scans ( $2 \text{ mV s}^{-1}$ ) recorded in  $0.1 \text{ M HClO}_4$  for the Pt/C electrodes and for the carbon support, denoted as C, only. Obviously, C is much less active than the sample with additional Pt. This confirms the negligible contribution of the support, despite its higher surface area.

### S3. Description of electrochemical cell and measurement procedure

A schematic of the cell utilized for the EIS measurements is shown in **Figure S4**. Noteworthy, a shunt capacitor,  $C = 4.2 \text{ } \mu\text{F}$ , was connected between the reference electrode and counter electrode to compensate potentiostat-caused artifacts at high frequencies.

EIS measurements were conducted after activating the catalysts. For the catalyst thin films, the activation was performed by potential cycling between  $0.93 \text{ V}$  and  $1.73 \text{ V}$  for three times ( $50 \text{ mV s}^{-1}$ ). In the case of nanoparticles, the potential was cycled between  $0.06 \text{ V}$  and  $1.20 \text{ V}$  until a stable CV was achieved. After the last cycle, the potential was swept ( $1 \text{ mV s}^{-1}$ ) to the starting potential of the first impedance measurement. We suggest to start the EIS measurements at least  $30 \text{ mV}$  below the potential shown in **Table 2** and increase it stepwise ( $10 \text{ mV}$  steps). Further, we suggest a frequency range between  $30 \text{ kHz}$  and  $10 \text{ Hz}$  (at least 60 points should be recorded) and a probing signal amplitude of  $\sim 10 \text{ mV}$ .

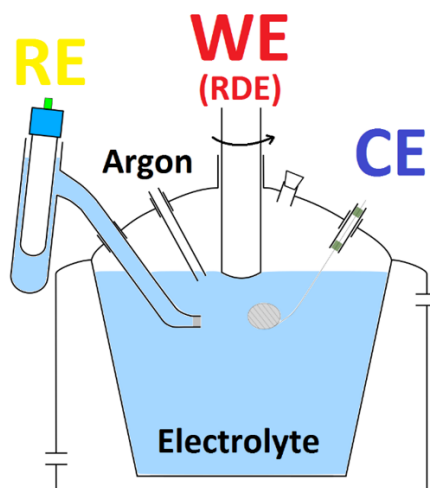


**Figure S4.** Schematic of the glass cell utilized for the electrochemical measurements. The double-walled cell allows temperature control of the electrolyte. A typical three-electrode configuration was utilized: reference electrode RE (MMS: Schott, Germany / RHE: Gaskatel, Germany), and counter electrode CE (Platinum mesh: Goodfellow, Germany) and an RDE tip as working electrode mounted on a rotator (Pine, USA). A shunt capacitor of  $4.2\ \mu\text{F}$  was connected between counter and reference electrode for EIS measurements. Ar saturated 0.1M KOH and 0.1M  $\text{HClO}_4$  were utilized as electrolytes.

## References

- 
- [1] Lasia, A. Electrochemical Impedance Spectroscopy and its Applications, *Springer, New York*, **2014**
  - [2] Harrington, D.A.; Conway, B.E. AC impedance of Faradaic reactions involving electrosorbed intermediates—I. Kinetic theory. *Electrochimica Acta* **1987**, 32, 1703-1712.
  - [3] Freakley, S.J.; Ruiz-Esquiús, J.; Morgan, D.J. The X-ray photoelectron spectra of Ir,  $\text{IrO}_2$  and  $\text{IrCl}_3$  revisited. *Surf. Interface Anal.* **2017**, 49, 794-799
  - [4] Pfeifer, V.; Jones, T. E.; Velasco Vélez, J. J.; Massué, C.; Arrigo, R.; Teschner, D.; Girgsdies, F.; Scherzer, M.; Greiner, M. T.; Allan, J.; Hashagen, M.; Weinberg, G.; Piccinin, S.; Hävecker, M.; Knop-Gericke, A.; Schlögl, R. The electronic structure of iridium and its oxides. *Surf. Interface Anal.* **2016**, 48, 261-273
  - [5] Watzele, S.; Liang, Y.; Bandarenka, A.S. Intrinsic activity of some oxygen and hydrogen evolution reaction electrocatalysts under industrially relevant conditions. *ACS Appl. Energy Mater.* **2018**, 1, 4196-4202